Accessibility and occlusion of biopolymers, ray tracing of radiating tubes, and the temperature of a tangle

Gregory Buck,[1,*] Robert G. Scharein,[2,†] Jeffrey Schnick,[3,‡] and Jonathan Simon[4,§]
[1]*Department of Mathematics, St. Anselm College, Manchester, New Hampshire 03102, USA*
[2]*Department of Computer Science, University of British Columbia, Vancouver, British Columbia, Canada V6T 1Z4*
[3]*Department of Physics, St. Anselm College, Manchester, New Hampshire 03102, USA*
[4]*Department of Mathematics, University of Iowa, Iowa City, Iowa 52242, USA*
(Received 22 November 2006; revised manuscript received 29 October 2007; published 23 January 2008)

We introduce a measure of complexity, an energy, for any conformation of filaments. It is the *occlusion*, the portion hidden when viewed from an arbitrary exterior point. By inverting we get the *exposure*, a first approximation of the *accessibility* of the filaments. Assuming the filament is a source, we get the *self-irradiation*, which leads to both an interpretation as the *temperature* and a visualization technique: ray tracing as a virtual laboratory. There is a wide variety of applications, from enzyme action on and radiation damage of biopolymers, to the geometry of light bulb filaments. Energy minimization provides automatic detangling, resulting in symmetric and pleasing conformations.

DOI: 10.1103/PhysRevE.77.011803 PACS number(s): 82.35.Lr, 02.10.Kn, 61.80.Az, 82.39.Pj

I. INTRODUCTION

There are many scientific reasons for studying the geometric and topological qualities of arrangements of filaments in three dimensions. To give an idea of the breadth of applications we mention just two. First, topology has become a fundamental tool in the study of the dynamics of polymers in general and of that most important polymer, DNA, in the specific. Second, at a considerably different scale, the topology of magnetic flux tubes in the solar corona is an important factor in solar dynamics. A natural conception is that of the complexity of the arrangement—we think of a single linear filament as simple or low energy, while a tangled ball of a filament or filaments is complex or high energy [1–9].

II. DERIVATION OF $E(K)$

We begin with the radiating tube interpretation, and derive the others from it. By the cosine law of radiation, the self-radiation of a radiating tube T is given by

$$\sigma(T) = 1/4\pi \int \int_{T\times T} (dA \sin \alpha)(dB \sin \beta)/\rho^2.$$

Here dA,dB are area elements for the surface of the tube and $\alpha\beta$ are the angles the separation vector makes with the surface of the tube (this is the cosine law—we are using the sine of the complementary angle). This formula makes sense for any non-self-intersecting tube. For a relatively thin tube, which is relatively far from self-intersection, it is natural to suppose that the self-radiation of the filament (a surface to surface integral) can be approximated by a double integral over the center curve K of the tube (a curve to curve integral). Let $C(x)$ denote a cylinder element about the point x that is a section of T of small but nonzero length. Then we consider the interaction between $C(x)$ and $C(y)$. (See Fig. 1.) First we note that if we consider $C(x)$ to be a point source, then the effect on $C(y)$ depends approximately on the angle the line element dy makes with $r=(x-y)/|x-y|$, since this determines the solid angle subtended by $C(y)$. On the other hand, $C(x)$ is not a point source, but emits through the cylindrical surface. The cosine law dictates that the intensity of the emission depends approximately on $|dy\, Xr|$. Of course, the surface area of the tube depends on the radius R of the tube, so we expect that $\sigma(T)=f(R)E(K)$, where the leading term in the coefficient function $f(R)$ is R^2, and

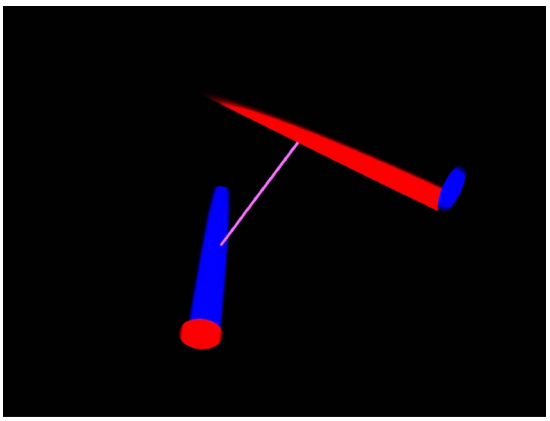

FIG. 1. (Color online) Tube geometry. Let the upper cylinder (red exterior in color image) be the tube element $C(x)$, the lower (blue) $C(y)$. The thin connecting cylinder between $C(x)$ and $C(y)$ is the separation vector r. [In the color image $C(x)$ is a source of blue light, which is why $C(y)$ is blue, as is the interior of $C(x)$. The exterior of $C(x)$ is red because it is reflecting the red light emanating from $C(y)$].

*Author to whom correspondence should be addressed. gbuck@anselm.edu
†scharein@cs.ubc.ca
‡jschnick@anselm.edu
§jsimon@math.uiowa.edu

$$E(K) = 1/4\pi \int \int_{K\times K} |dx\, Xr||dy\, Xr|/\rho^2.$$

$E(K)$ is our measure. We have done some preliminary numerics on simple cases and found what we would expect: That the surface integral does become proportional to this line integral in the limit as the radius of the tube shrinks. Formal numerics and estimates of the "error" engendered by using the line integral will be the object of further study.

Now let $C(x)$ and $C(y)$ be sufficiently far apart, and again let $C(x)$ be a point. Then how much $C(y)$ tends to obscure $C(x)$ depends on its orientation with respect to $C(x)$. [If the angle between dy and r is zero, then to first approximation the surface of $C(y)$ does not obscure $C(x)$ at all—from a viewpoint along r ["behind" $C(y)$], one sees $C(x)$ through the center of $C(y)$.] On the other hand, since $C(x)$ is in fact a cylinder, how much of the surface of $C(x)$ is occluded by $C(y)$ also depends on the angle between dx and r—again, if this angle is zero then none of the surface of $C(x)$ is occluded. Note that this is a directional occlusion—a patch blocked from an oblique angle has a lesser contribution.The exposure of a linear tube is proportional to LR, where L is the length of the tube, so the exposure of an arbitrary conformation is proportional to $mLR-f(R)E(K)$ (m being a constant). Now imagine a filament requiring an agent to act at a

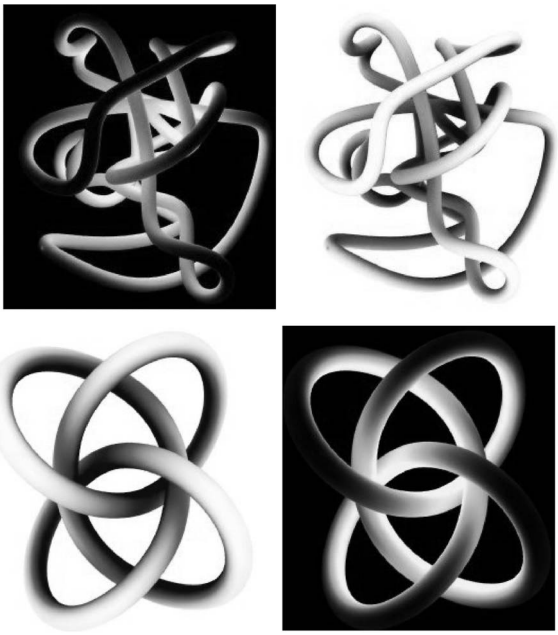

FIG. 2. Occlusion and accessibility as the "inverse" of self-radiation and temperature. 2*A* (self-radiation) was created via ray-tracing. 2*B* is simply the inverse image via Photoshop, and accessible regions are light colored, occluded ones are "shadowed." This illustration was suggested by Felice Frankel.

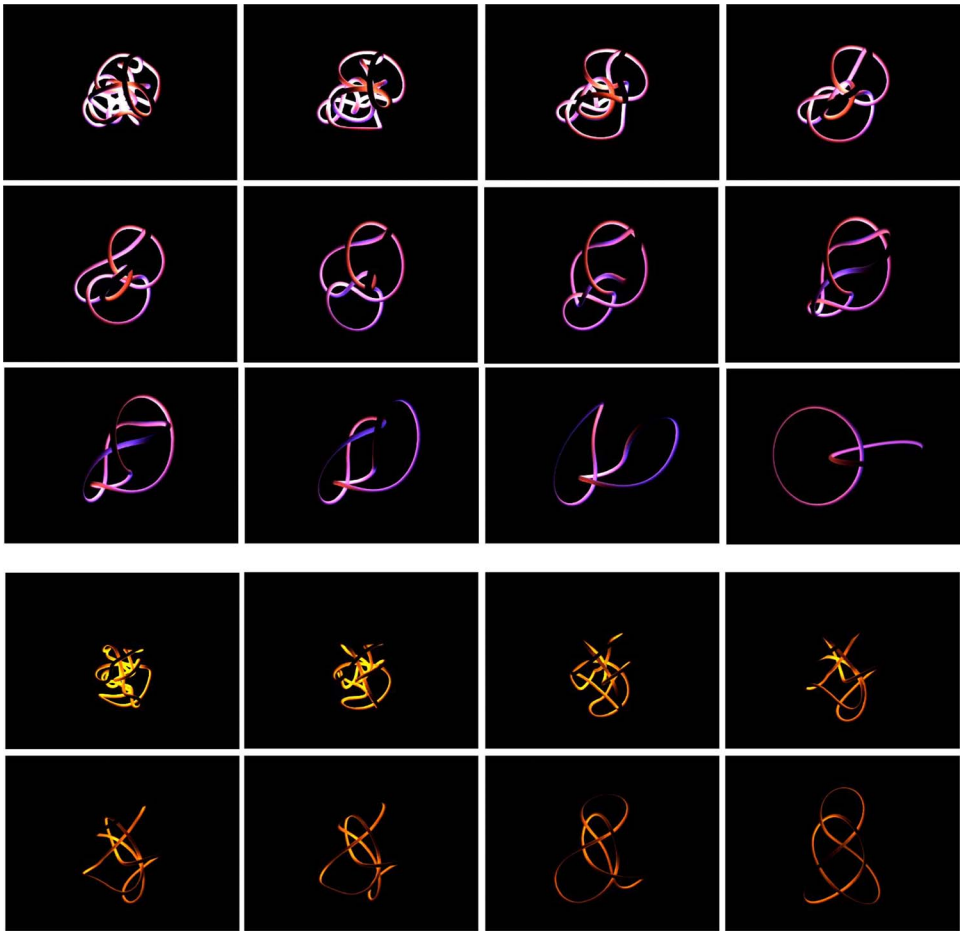

FIG. 3. (Color online) Simplification of complex conformations to canonical forms by the gradient flow of E.

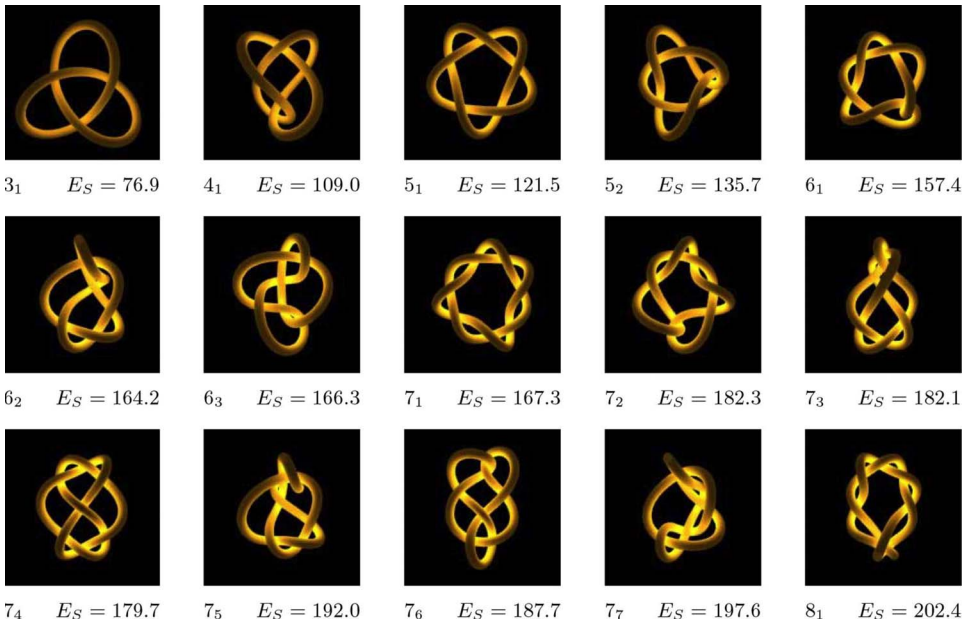

FIG. 4. (Color online) Apparent energy minimums for some simple knot and link types.

particular site or sites. Then it is reasonable to suppose that the ease which the agent can act depends on how exposed or obscured the site is from an average viewpoint—if the arrangement is complex, it may be more difficult (take longer) for the agent to reach interior sites. One can think of the exposure as the sum of the straight line paths from a large sphere enclosing the filamentary molecule to sites on the filament, and so it is a reasonable first approximation of accessibility. The "inverse" relationship between occlusion and exposure (self-irradiation) is easy to illustrate graphically. See Fig. 2.

III. APPLICATIONS IN BIOLOGY

Radiation damage is of central importance in DNA dynamics, as it can create mutations and terminate replication. It is plausible that regions with greater exposure in packings would undergo more mutations (so are less conserved) than those with less exposure. So we might expect a correlation between conservation and exposure at a point along the DNA strand [the interior integral of $E(K)$]. This would help explicate the design and role of chromatin [10,11].

Furthermore, during replication the strand needs to be exposed or accessible at the replication fork in order to build the base pairs. So as replication proceeds $E(K)$ is locally decreased along the strand, then increased as the strands are packed.

The detangling of DNA daughter strands that is necessary for cell division is accomplished by the topoisomerase enzymes. In particular, type 2 topoisomerase passes one double helix though another. If the strands are tightly packed, and so have high E, this procedure is as likely to increase entanglement as to decrease it. And so we expect topoisomerase type 2 to be most effective in detangling in low E conformations. Moreover, the enzyme itself is rather large, and so the speed at which it can search for sites to act upon may be restricted by the accessibility [12–14].

There has been considerable progress made in modeling enzyme search patterns in general. Enzymes may employ sliding along the strands, or jumping from strand to strand or combinations of techniques. The relative efficiencies of the strategies depend in general on a geometric factor of the conformation that measures the accessibility. In this case greater occlusion means that it is easier for an enzyme to find another strand nearby, so jumping from strand to strand is good strategy [15,16].

IV. APPLICATIONS IN PHYSICS

Imagine two tubes of equal length and radius, made of perfect conductors. They are heated, in a vacuum, to some specific temperature, and then allowed to cool. If one tube is a linear tube, and the second a complex arrangement, then we would naturally expect the linear tube to have a faster rate of cooling—conversely we wrap our arms around ourselves to keep warm. Now let the conformation be a filament in which thermal energy is produced at a fixed rate, as in the case of a 60 W light bulb in which electrical energy is converted into thermal energy at a rate of 60 J/s. Upon reaching thermal equilibrium, such a filament radiates energy into space at the same fixed rate. In the case of a complex knot, as compared to a simple knot, much of the energy radiated by the filament is redeposited in the filament as a result of self-irradiation. In order to radiate energy into space at the prescribed rate, each unit area of the filament must radiate energy at a greater rate than it would in the case of a simple knot. To do so, the filament must be at a higher temperature. Heuristically, one way to approach this is to say that increasing the complexity of the conformation in a sense reduces the effective surface area—for example if the complexity is high enough one could imagine stations near the center of

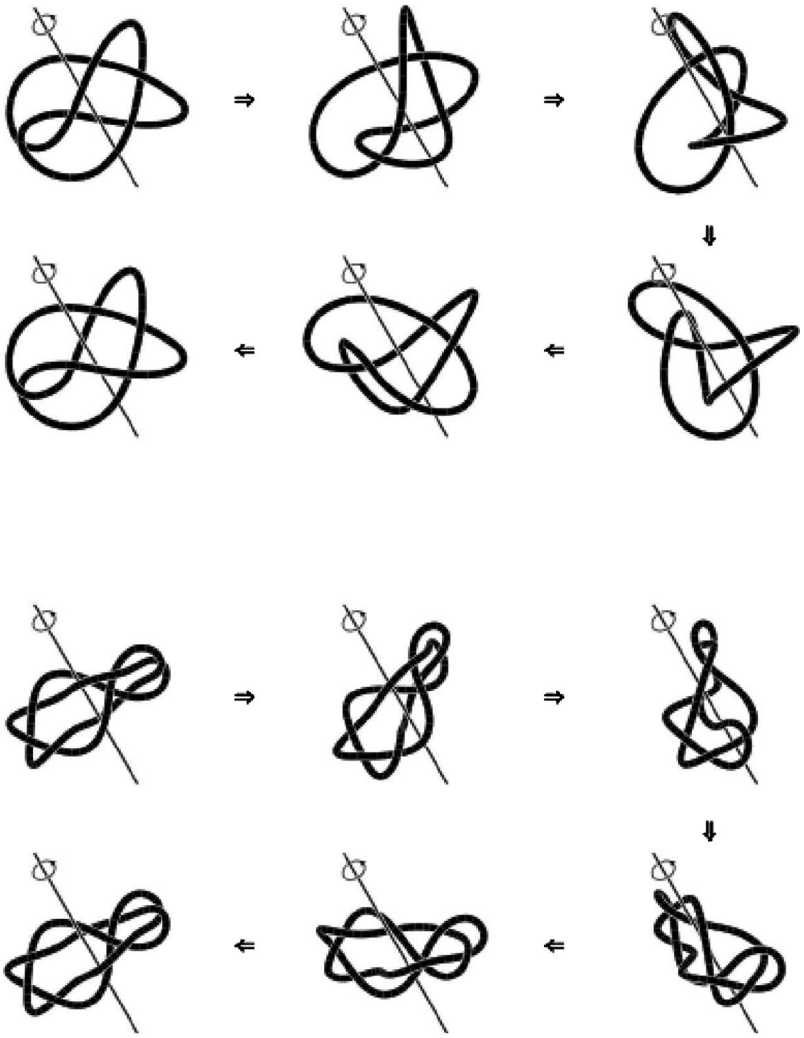

FIG. 5. Symmetry of figure 8 canonical conformation (energy minimum). Symmetry of 8_3 energy minimum. These are rigidly achiral knots—they are topologically equivalent to their mirror images, and this is shown by rigid rotations of the canonical conformations.

the conformation which have no direct line path reaching the exterior. So, on average, more energy has to emanate from each unit of surface. Designers of incandescent light bulb filament geometries take care to avoid "hotspots"—places where the filament is too close to itself—uneven distribution of heat creates weak spots. So a good geometry has high E from compactness but equidistribution of the self-irradiation. Helices have this property and are the most common design. Compact fluorescent bulbs have similar design requirements and also employ helices.

V. VISUALIZATION AND CALCULATION

To visualize $E(K)$, we use the computer graphics technique of ray-tracing, which mimics the basic laws of light, as a virtual laboratory. In ray-tracing, the image is created by following the idealized paths of light rays as they impinge on the three dimensional scene. The technique can result in realistic appearing images, since it can model complicated phenomena such as reflection, diffusion, and opacity of surfaces. In Fig. 1, the light source is distributed along the center curve of the knot, and the tube is a light filter (like frosted glass) so that the surface both emits and reflects. Therefore, the intensity of the reflected light represents the energy: The more complicated knot is brighter. *Note that this technique is not a coloring scheme, it is an embodiment of the radiation interpretation of the energy*. The technique is in some sense "proved" by watching the gradient descent evolutions—the conformations become dimmer as they simplify. See Fig. 2. The surface of the tube has differential brightness: Near self-crossings are brightly illuminated, strands with low curvature far removed from other strands are barely illuminated (a simple linear cylinder has zero energy). With links, we can use different color lights to demonstrate the effect of one link upon itself and another. In general, we can read off complexity from the overall intensity of the conformation. This visualization technique can likely be applied to other problems, in particular to models of surface accessibility of surfaces of arbitrary shape. So it could be used in several aspects of molecular analysis.

Both $E(K)$ and its gradient are relatively easy to compute (approximate) numerically. We have conducted many numerical experiments, on many knot and link types, beginning with many different initial conformations. The experiments were conducted on Silicon Graphics computers, utilizing the software KnotPlot (9—software written by one of the authors—Scharein).

As with other inverse distance knot energies, simple gradient descent seems to be almost unreasonably effective in

simplifying high energy (complicated) initial conformations [9,17]. In fact each prime knot type seems to have just one (global) minimum energy conformation; no local minima have been found. See Fig. 3. In fact, we issue a general challenge: Find a prime knot conformation that is not carried to a global minimum by the gradient (for reasons other than simple computational complexity). Computing E is an N^2 computation, where N is the number of edges in the polygonal approximation of the curve, so entanglements of considerable complexity are tractable.

The minimum energy conformations have various symmetries (see Fig. 4). Some of these are subtler than one might expect. For example, the minimal conformation of the figure eight knot, one of the relatively rare achiral knots, reveals the achirality: A rigid rotation of the conformation and the mirror image of the conformation can be superimposed. This is also the case with minimum energy conformation of the knot known as 83, another achiral knot. (See Fig. 5).

Galleries of images and animations are in Ref. [22]. The software KnotPlot is available in Ref. [23].

VI. $E(K)$ AND OTHER MEASURES OF CONFORMATIONAL COMPLEXITY

Elsewhere we have established the fundamental relationship of inverse square measures on curves, such as the writhe and the average crossing number to other elementary measures of complexity, such as the crossing number and the rope length of the conformation [1–4]. E is an inverse square measure, so has this relationship. The average crossing number is a modification of Gauss's linking number [5]. It measures how much, on average, the filament appears to cross itself from an arbitrary viewpoint (in a given conformation). We note that the average crossing number (ACN) cannot be used as an energy in our sense, it is finite on self-intersecting curves and therefore conformations may change knot type under gradient flow.

It is straightforward to show that E bounds the ACN; see [1,4]. Since the ACN, being an average, bounds the crossing number of a knot or link (the minimal number of crossings required in a planar diagram of the topological type), E bounds the crossing number as well. Grassberger [21] put forward that the ACN measures what he termed opacity—distinguishing this from entanglement, since it is certainly possible to have high ACN and no entanglement. The ACN can be looked at as an upper bound on entanglement. Under this interpretation the self-radiation (the "inverse" of the occlusion) bounds, but is not equal to, the opacity.

The ropelength is the shortest length of a unit radius tube that can realize a topological type. We have shown [4] that 11 rope length $(K)^{4/3} \geq E(K)$, and that the exponent in this bound cannot be improved.

The bound on the ACN allows us to relate $E(K)$ to physical measures arising from field considerations. [Note that three-dimensional field quantities are often not amenable to numerical approximation because of the size of the computations, but $E(K)$ is.] The helicity of a vector field, a construction due to Moffat, is given by $H=\int_D \mathbf{A}\cdot\mathbf{B}\, dV$, where $\mathbf{B}$ is the vector field, $\mathbf{A}$ is a vector potential, and D is the region containing $\mathbf{B}$ (say a flux tube). In the case where the flux tubes have circular cross section of constant radius and the field is twist free, it has been shown that helicity $=\text{flux}^2$ writhe(K), where K is the center curve of the tube [see [18,19]; a rigorous proof appears in [20]]. But the writhe is bounded by the ACN, so in this case we have that $E \geq \text{helicity}/\text{flux}^2$.

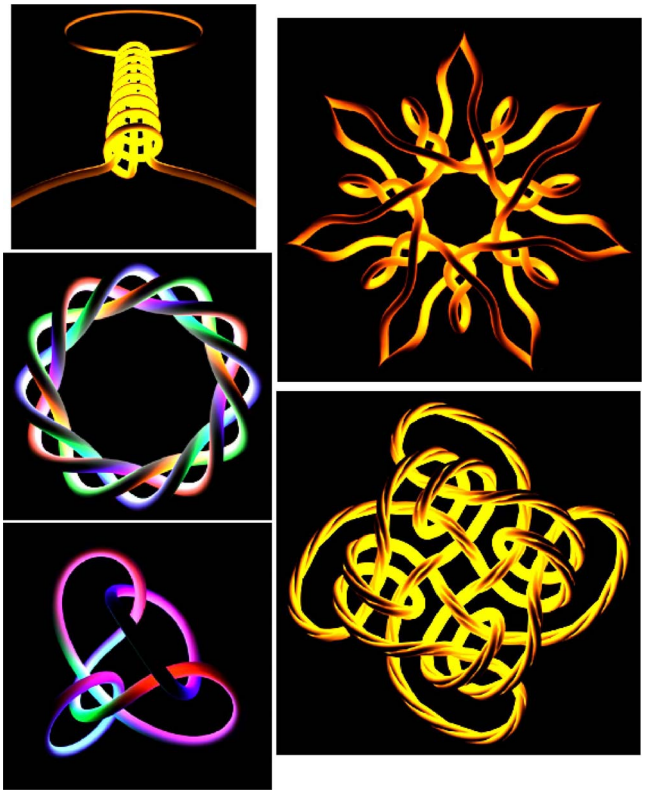

FIG. 6. (Color online) Ray-traced radiating tube pictures, including a coil conformation like a light bulb filament. In the multicolored images, each component (closed loop) radiates a different color light.

As a fundamental measure of the three-dimensional conformational complexity of filaments, $E(K)$ has three attractive qualities: It is defined as an integral over the curve (and so is amenable to computation), is singular on self-intersecting knots (and so separates knot types by infinite potential walls), and it has real biological and physical interpretations.

ACKNOWLEDGMENTS

The authors are supported in part by NSF Grants No. DMS9407132 and No. DMS9420088.

[1] G. Buck, Nature (London) **392**, 238 (1998).
[2] G. Buck and J. Orloff, Topol. Appl. **61**, 205 (1995).
[3] G. Buck and J. Simon, *Lectures at Knots '96*, edited by S. Suzuki, International Conference on Knot Theory, Tokyo, 1996 (World Scientific, Singapore, 1997), pp. 219–235.
[4] G. Buck and J. Simon, Topol. Appl. **91**, 245 (1999).
[5] M. Freedman, Z.-X. He, and Z. Wang, Ann. Math. **139**, 1 (1994).
[6] H. K. Moffatt, Nature (London) **347**, 367 (1990).
[7] J. O'Hara, Topology **30**, 241 (1991).
[8] Katritch *et al.*, Nature (London) **384**, 142 (1996).
[9] R. Scharein, Knot-Plot, Program for drawing, visualizing, manipulating, and energy minimizing knots, Univ. British Columbia, www.cs.ubc.ca/spider/scharein/
[10] H. Leonhardt *et al.*, J. Cell Biol. **149**, 271 (2000).
[11] K. P. Lemon and A. D. Grossman, Science **282**, 1516 (1998).
[12] V. V. Rybenkov, C. Ullsperger, A. V. Vologodskii, and N. R. Cozzarelli, Science **277**, 690 (1997).
[13] J. Yan, M. O. Magnasco, and J. F. Marko, Nature (London) **401**, 932 (1999).
[14] G. Buck and E. Lynn Zechiedrich, J. Mol. Biol. **340**, 933 (2004).
[15] O. G. Berg, R. B. Winter, and P. H. von Hippel, Biochemistry **20**, 6929 (1981).
[16] S. E. Halford, Biochem. Soc. Trans. **29**, 363 (2001).
[17] K. Brakke, The Surface Evolver, software available at http://www.susqu.edu/brakke/
[18] M. A. Berger and G. B. Field, J. Fluid Mech. **147**, 133 (1984).
[19] M. A. Berger, Plasma Phys. Controlled Fusion **41**, B167 (2000).
[20] H. K. Moffatt and R. Ricca, Proc. R. Soc. London, Ser. A **439**, 411 (1992).
[21] P. Grassberger, J. Phys. A **34**, 9959 (2001).
[22] http://www.knotplot.com/se/
[23] http://www.knotplot.com